Chemical solution deposition of thin films for protonic ceramic fuel cells

Per Martin Rørvik [a,*], Camilla Haavik [a], David Griesche [b], Theodor Schneller [b], Filip Lenrick [c], L. Reine Wallenberg [c]

[a] SINTEF Materials and Chemistry, Box 124 Blindern, 0314 Oslo, Norway

[b] Institut für Werkstoffe der Elektrotechnik II, RWTH Aachen University, D52056 Aachen, Germany

[c] Centre for analysis and synthesis / nCHREM, Lund University, Box 124, S-221 00 Lund, Sweden

* Corresponding author: Per Martin Rørvik

Tel.: +47 93234039

Email address: per.martin.rorvik@sintef.no

Postal address: SINTEF Materials and Chemistry, P.O. Box 124 Blindern, 0314 Oslo, Norway

Abstract

Chemical solution deposition (CSD) offers the opportunity to fabricate very thin electrolyte films at lower temperatures than traditional powder-based methods. CSD methods have not been used much in production of protonic ceramic fuel cells (PCFC) until now. In this contribution we describe thin film deposition of the two proton-conducting materials $BaZr_{0.9}Y_{0.1}O_{3-\delta}$ (BZY) and $La_{28-x}W_{4+x}O_{54+\delta}$ (LWO) by spin coating. BZY films deposited on single-crystalline MgO grew epitaxially on the substrate. On a realistic PCFC cermet anode, 800 nm thick BZY films could be fabricated with a columnar structure which is promising to circumvent the low conductivity at grain boundaries of BZY. LWO films with some porosity were deposited on platinized Si from an aqueous solution.

Keywords: Spin coating, thin film, proton conductors, TEM, BZY, lanthanum tungstate

1. Introduction

Ceramic fuel cells with proton-conducting electrolytes are promising for fuel cells operating at 400-600 °C due to the relatively low activation energy for proton conduction (about 0.3–0.6 eV) and the efficient fuel utilization [1]. At these operating temperatures it is desirable to use thin electrolytes and nanoscaled cathodes to enhance the fuel cell performance. The relatively low operating temperature makes it possible to also use lower fabrication temperatures than traditionally used for ceramics, which have several benefits: nanoscale structuring of porous electrodes is easily achieved, cheaper metallic supports can be used instead of ceramic ones, harmful interface reactions are reduced, and less thermal energy is needed in the production process. Lowering of the fabrication temperature while at the same time obtaining dense thin electrolytes necessitates physical or chemical deposition methods as traditional methods typically requires temperatures well above 1000 °C. The fabrication temperature should however be high enough to obtain phase-pure materials without organic residue and to establish good ionic contact between the electrolyte and the electrode, and between the electrode grains. The reduced diffusion at lower temperatures may also make it necessary to use longer time at the maximum fabrication temperature compared to higher fabrication temperatures.

Chemical solution deposition (CSD) methods can be used to lower the fabrication temperature for protonic ceramic fuel cells (PCFC). CSD technology generally involves applying a homogeneous solution onto an underlying material, followed by drying to remove the solvent, pyrolysis annealing and crystallization annealing. To achieve films of appropriate thickness several layers are often deposited and the annealing is then typically done in a diffusion or rapid thermal processing furnace to save time and to control the densification and nucleation processes [2]. CSD methods have been used widely for oxide ion-conducting ceramic fuel cells [3], but in PCFC processing there are few reports. Proton-conducting electrolyte thin films of $BaCeO_3$ [4], $BaCe_{0.8}Gd_{0.2}O_{3-\delta}$ [5], $BaZr_{1-x}Y_xO_{3-\delta}$ [6-8], $SrZr_{1-x}Yb_xO_{3-\delta}$ [9], $SrCe_{0.95}Yb_{0.05}O_{3-\delta}$ [10] and $Sr_3CaZr_{0.5}Ta_{1.5}O_{8.75}$ [11] have been reported in the literature. For PCFC cathodes, infiltration into a porous backbone [12-15] and spray pyrolysis [14] have been used. Here we demonstrate CSD of two proton-conducting materials: $La_{28-x}W_{4+x}O_{54+\delta}$ (LWO), from an aqueous solution, and BZY, from a propionic acid-based solution. LWO is an alternative to the alkaline earth cerates or zirconates and exhibits a relatively pure proton conduction at low and intermediate temperatures which is useful as an electrolyte in PCFC [16,17]. BZY is one of the most promising electrolytes for PCFC due to its high chemical stability and relatively high bulk proton conductivity [1]. Here we demonstrate CSD of BZY on a cermet anode to show the feasibility of CSD fabrication of PCFC at a relatively low fabrication temperature of 1000 °C.

2. Experimental

$La_{28-x}W_{4+x}O_{54+\delta}$ (LWO) electrolyte thin films were deposited from an aqueous solution stabilized with either citric acid or ethylenediaminetetraacetic acid (EDTA) as chelating agent. $La(NO_3)_3{\cdot}9H_2O$ (99%, Merck) was dissolved in water followed by citric acid (anhydrous, 99.5%, SAFC) or EDTA (99%, Acros Organics) addition. NH_4OH (32 wt%, Merck) was added to obtain a neutral pH, resulting in the formation of a white gel-like substance that dissolved after several hours of stirring. WO_3 (99.9%, Fluka) was dissolved in NH_4OH by stirring at 75 °C for several hours followed by citric acid or EDTA addition. The La and W solutions were standardized by thermogravimetry and mixed to obtain the

desired La/W atomic ratio, typically La/W = 5.5 ($La_{5.5}WO_{11.25}$, LWO). The cation:citric acid or cation:EDTA molar ratio was 1:1 and the total salt concentration of the final solutions was 0.66 mol·L^{-1} for the citric acid solution and 0.45 mol·L^{-1} for the EDTA solution. Thin films were deposited by multiple spin coatings onto a platinized Si substrate ($Pt/TiO_x/SiO_2/Si$), with intermediate pyrolysis on a hotplate at 200 °C and then 500 °C. Before deposition of the first layer the substrate was heat-treated at 200 °C for 2 min on a hotplate and cooled to room temperature, to improve the adherence of the aqueous solution to the substrate. After the desired number of layers had been deposited the film was crystallized by annealing in a muffle furnace (heating rate 3 K·min^{-1}) or by rapid thermal processing (RTP, 200 K·min^{-1}).

$BaZr_{0.9}Y_{0.1}O_{3-\delta}$ (BZY) electrolyte thin films were deposited from a modified propionic acid-based solution described in [6]. First stoichiometric amounts of $BaCO_3$ (99.997 %, Alfa Aesar) and $Y(OOCCH_3)_3{\cdot}4H_2O$ (99.99 %, Alfa Aesar) were dissolved at elevated temperature in a mixture of propionic acid (f. s., Merck) and propionic acid anhydride (f. s., Merck). The propionic acid anhydride was added to remove the crystal water of the acetate precursor. In the second step $Zr(OCH_2CH_2CH_2CH_3)_4{\cdot}HOCH_2CH_2CH_2CH_3$ (Alfa Aesar) was diluted with anhydrous *n*-butanol (p. a., Merck) and stabilized with two equivalents of acetylacetone (p. a., Merck). The two solutions were mixed and filled up to reach an A cation concentration of 0.3 mol·L^{-1} in the final precursor stock solution. The deposition was performed by spin coating onto single crystalline MgO(100) or composite anodes ($BaCe_{0.2}Zr_{0.7}Y_{0.1}O_{3-\delta}$ (BCZY27) 35 wt% - NiO 65 wt%, supplied by CoorsTek) followed by a one-step thermal treatment in a diffusion furnace after each deposition cycle at temperatures of 800-1000 °C.

Basic microstructure characterization of the LWO films was done by scanning electron microscopy (SEM, FEI Nova NanoSEM 650). For advanced characterization a (scanning) transmission electron microscope ((S)TEM, JEOL 3000F) equipped with X-ray energy-dispersive spectroscopy (XEDS), high angle annular dark field (HAADF) and energy-filtered TEM (EFTEM) was used. TEM specimens were prepared by focused ion beam machining (FEI Nova NanoLab 600). The phase composition was studied by grazing incidence X-ray diffraction (GIXRD, Bruker AXS D8 Discover).

3. Results and Discussion

For deposition of the LWO films, two chelating agents were evaluated for stabilization of La and W in the aqueous solution: citric acid and ethylenediaminetetraacetic acid (EDTA). The LWO films from citric acid solution became crystalline after annealing at 800 °C or above (Fig. 1), while at lower temperatures the films were mostly amorphous. The diffractograms correspond well to the pattern of La_6WO_{12} (PDF number 30-686) and to the diffractograms for lanthanum tungstate with La/W atomic ratio 5.5 reported by Magraso *et al*. [18].The diffractogram of the film annealed at 800 °C for 10 min indicates a small amount of La_2O_3 present in the film, but further annealing (30 min) produced single-phase LWO. The TEM images in Fig. 2 show the small grain size (10-20 nm) of the film annealed at 800 °C for 30 min and the individual layers can be seen. It is clear that the film contains layered pores as seen by the brighter areas in the TEM image. Lower magnification SEM images revealed that the films tended to crack or form circular craters during annealing at 600 °C and above, with more craters being formed with increasing temperature. The origin is probably incomplete burnout of organic residue in the intermediate pyrolysis on the hotplate between each layer; also, citrate

compounds can undergo an explosive decomposition. As a result the films could not be densified further by increasing the annealing temperature as it resulted in an increase in the number of cracks and craters.

To avoid the crater formation, citric acid was replaced by EDTA. The LWO films deposited from EDTA solution were more homogeneous than the citric acid-deposited films and craters were not observed. A thickness of about 350 nm was achieved after 10 successive depositions (Fig. 3). Annealing at 800 °C for 4 h led to a polycrystalline LWO film with nanoscaled grains (20-60 nm). The film had some porosity especially in the in-plane direction reflecting the multi-layer deposition. Final annealing at higher temperatures generally led to substantial grain growth and formation of larger pores instead of densification. Initial measurements for determining the through-plane conductivity was unsuccessful due to short-circuiting, probably due to cracks in the film, open porosity, or mechanical failure as the top electrode was applied. Thus, for use as a gas-tight electrolyte the density has to be improved; further optimization of the processing conditions is necessary to achieve completely dense LWO films, such as a lower concentration of the solution, intermediate crystallization annealing at 800 °C or above between each layer, and the use of a shrinking substrate such as an unsintered ceramic. However, the time used for deposition of a LWO with a certain thickness will inevitably increase with these implementations.

BZY thin films were also deposited. First, BZY was deposited on single-crystalline MgO substrates. The BZY film had an epitaxial interface to the MgO substrate as the lattice match between BZY and MgO is very good. The film was monolithic and without grain or twin boundaries. For the BZY film annealed at 1000 °C, imaging in scanning TEM mode showed a layered pattern of higher intensity in the single-crystal film (Fig. 4). This was attributed to regularly occurring voids, which possibly originates from incomplete removal of carbonate species during the initial crystallization of that layer followed by removal at later crystallization steps. A detailed electron microscopy study of the BZY films on MgO is reported in ref. [7]. Measurements of the in-plane conductivity are in progress and will be reported later.

In a real fuel cell the electrodes naturally have to be porous to allow gas transport towards the electrolyte. It is challenging to deposit a thin, even and dense film onto a porous support, especially if the pores are large. Solutions to this challenge can be to minimize the pores in the electrode closest to the electrolyte by reducing electrode grain size, to clog the pores with electrolyte phase grains [19] or a polymer film [5], to deposit thicker films that more easily cover the pores, or to introduce the pores after electrolyte deposition. The last option is probably the easiest when using a NiO-electrolyte material cermet as anode; the NiO of the cermet is reduced to Ni in reducing atmosphere at the operating conditions, which induces porosity for gas diffusion. The film can therefore be deposited onto a dense support. Fig. 5 shows an example of such a BZY film deposited onto a BCZY27-NiO anode and annealed at 1000 °C. The anode was not reduced before the TEM study so the anode was still dense. The film grew partly epitaxially on the BCZY anode grains but there was no epitaxial relationship between the NiO part of the substrate and the BZY film. As seen in Fig. 5b the BZY grains in the film were columnar; 20-100 nm in diameter and about 800 nm long (full film thickness). The columnar growth is a result of the crystallization between each layer to promote heterogeneous nucleation on the grains of the previous layer, instead of homogeneous nucleation in the deposited layer that would have given a random crystalline structure.

The columnar film structure should in principle avoid the problem of low proton conduction along the grain boundaries of BZY [20], as each grain stretches through the whole electrolyte thickness so that a proton traveling through the electrolyte do not have to pass any grain boundaries from the anode to the cathode side. The in-plane conductivity is however expected to be low due to the high number of grain boundaries in that direction. Previously, Pergolesi *et al*. demonstrated that grain-boundary-free BZY thin films show a very high proton conductivity of 0.11 $S \cdot cm^{-1}$ at 500 °C [21]; those BZY films were deposited onto MgO substrates by pulsed laser deposition and were epitaxially oriented. Due to the non-conducting MgO substrate their measurements were performed in-plane. For a practical fuel cell, columnar grain growth with partial epitaxial relation to the electrodes is more realistic than single-crystalline electrolyte films, as the latter are difficult to deposit onto functional anodes.

As a final comment, if dense thin films cannot be obtained by CSD, the porous structure can anyway be useful, for instance as catalytic surface layer or as a thin cathode backbone for infiltration. Porous thin films have also recently been shown to exhibit proton conduction at room temperature due to water adsorption [22] and CSD methods will be important for any practical use of this phenomenon.

4. Conclusions

A columnar BZY thin film with thickness of 800 nm was successfully deposited onto NiO-BCZY anode from a propionic acid-based solution. The columnar microstructure avoids the challenge of low grain boundary conduction in BZY and the BZY film should therefore be highly suitable as an electrolyte in a PCFC. On single-crystalline MgO substrate, the BZY film grew epitaxially on the substrate.

Deposition of LWO thin films on platinized Si from an aqueous solution was demonstrated. The films were not dense and further optimization of the CSD processing is needed for use as an electrolyte in PCFC. Using EDTA as stabilizer proved to be better than using citric acid as the prior gave smoother films.

Compared to traditional powder-based methods, CSD methods offer the opportunity to fabricate very thin electrolyte films (< 1 μm) at much lower temperatures ($\leq$ 1000 °C) but optimization of the solution chemistry and deposition procedure are vital.

5. Acknowledgements

This work was carried out within the nextgenFCmat project (Next generation fuel cell materials), financed through the Northern European Innovative Energy Research Programme (N-INNER II) by The Research Council of Norway (project nr. 197935), The Swedish Energy Agency (N-INNER D. nr 2010-000530 project nr. 32939-1) and Projektträger Jülich (BMBF grant nr. 03SF0392). The authors also thank CoorsTek Inc. in Golden Colorado for providing the cermet anode supports used in this study.

6. References

[1] E. Fabbri, D. Pergolesi, E. Traversa, Chem. Soc. Rev. 39 (2010) 4355-4369.
[2] R.W. Schwartz, T. Schneller, R. Waser, C. R. Chim. 7 (2004) 433-461.
[3] C. Haavik, P.M. Rørvik, in: T. Schneller, R. Waser, M. Kosec, D. Payne, (Eds.), Chemical Solution Deposition of Functional Oxide Thin Films, Springer, 2013, accepted for publication.
[4] E.M. Kelder, O.C.J. Nijs, J. Schoonman, Solid State Ion. 68 (1994) 5-7.
[5] V. Agarwal, M.L. Liu, J. Mater. Sci. 32 (1997) 619-625.
[6] T. Schneller, T. Schober, Solid State Ion. 164 (2003) 131-136.
[7] F. Lenrick, D. Griesche, J.-W. Kim, T. Schneller, L.R. Wallenberg, ECS Trans. 45 (2012) 121-127.
[8] K. Somroop, R. Pornprasertsuk, S. Jinawath, Thin Solid Films 519 (2011) 6408-6412.
[9] J. Eschenbaum, J. Rosenberger, R. Hempelmann, D. Nagengast, A. Weidinger, Solid State Ion. 77 (1995) 222-225.
[10] I. Kosacki, H.U. Anderson, Sens. Actuator B-Chem. 48 (1998) 263-269.
[11] C. Savaniu, J.T.S. Irvine, Solid State Ion. 150 (2002) 295-308.
[12] T.Z. Wu, Y.Q. Zhao, R.R. Peng, C.R. Xia, Electrochim. Acta 54 (2009) 4888-4892.
[13] F. Zhao, Q. Liu, S.W. Wang, F.L. Chen, J. Power Sources 196 (2011) 8544-8548.
[14] S. Ricote, N. Bonanos, P.M. Rørvik, C. Haavik, J. Power Sources 209 (2012) 172-179.
[15] S. Ricote, N. Bonanos, F. Lenrick, R. Wallenberg, J. Power Sources 218 (2012) 313-319.
[16] R. Haugsrud, C. Kjølseth, J. Phys. Chem. Solids 69 (2008) 1758-1765.
[17] A. Magrasó, J. Power Sources 240 (2013) 583-588.
[18] A. Magrasó, C. Frontera, D. Marrero-López, P. Núñez, Dalton Trans. (2009) 10273-10283.
[19] P. Jasinski, S. Molin, M. Gazda, V. Petrovsky, H.U. Anderson, J. Power Sources 194 (2009) 10-15.
[20] C. Kjølseth, H. Fjeld, Ø. Prytz, P.I. Dahl, C. Estournès, R. Haugsrud, T. Norby, Solid State Ion. 181 (2010) 268-275.
[21] D. Pergolesi, E. Fabbri, A. D'Epifanio, E. Di Bartolomeo, A. Tebano, S. Sanna, S. Licoccia, G. Balestrino, E. Traversa, Nat. Mater. 9 (2010) 846-852.
[22] B. Scherrer, M.V.F. Schlupp, D. Stender, J. Martynczuk, J.G. Grolig, H. Ma, P. Kocher, T. Lippert, M. Prestat, L.J. Gauckler, Adv. Funct. Mater. 23 (2013) 1957-1964.

Figure captions

Figure 1. X-ray diffractograms with grazing incidence θ = 1° of five LWO thin films deposited from citric acid solution. After the final layer deposition and pyrolysis the films were annealed for crystallization and sintering as indicated.

Figure 2. (a) TEM image and (b) high resolution TEM (HRTEM) image of LWO film deposited from citric acid solution, heat-treated at 800 °C for 30 min by RTP. A fast Fourier transform of the HRTEM image is displayed in inset showing a polycrystalline pattern corresponding to LWO without preferential orientation.

Figure 3. (a) SEM image of LWO thin film deposited from an EDTA-stabilized aqueous solution on platinized Si. 10 layers were deposited with pyrolysis at 500 °C on a hotplate between each layer. The film was finally crystallized at 800 °C for 4 h in air. (b) X-ray diffractogram with grazing incidence θ = 1° of the LWO thin film imaged in (a).

Figure 4. STEM bright field image of an epitaxial BZY film on MgO annealed at 1000 °C. The regular STEM-brighter spots are volumes of lower density (voids), in an otherwise monolithic (single crystal) matrix.

Figure 5. (S)TEM images of BZY film deposited by CSD (20 layers) on a dense BCZY27-NiO anode and annealed at 1000 °C. (a) Overview STEM HAADF image. (b) Higher magnification TEM image of the columnar BZY growth on a NiO part of the anode.

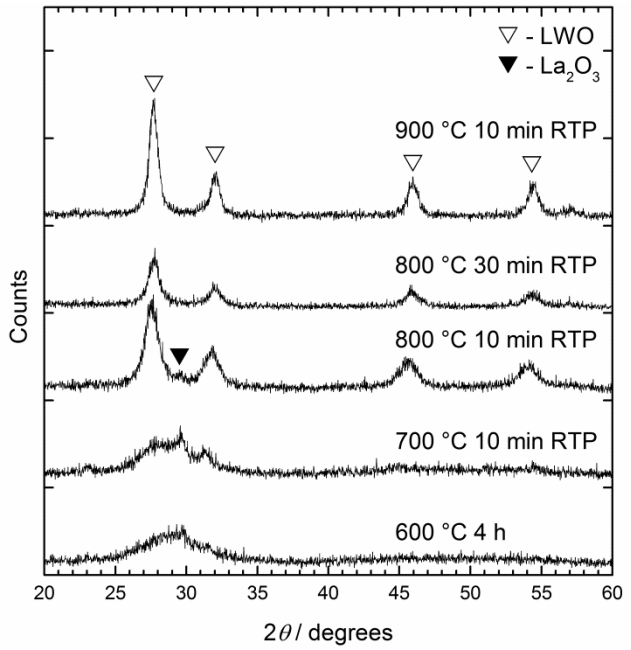

Figure 1. X-ray diffractograms with grazing incidence θ = 1° of five LWO thin films deposited from citric acid solution. After the final layer deposition and pyrolysis the films were annealed for crystallization and sintering as indicated.

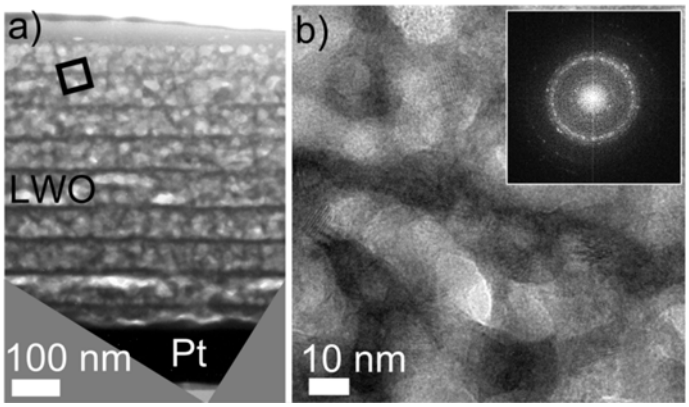

Figure 2. (a) TEM image and (b) high resolution TEM (HRTEM) image of LWO film deposited from citric acid solution, heat-treated at 800 °C for 30 min by RTP. A fast Fourier transform of the HRTEM image is displayed in inset showing a polycrystalline pattern corresponding to LWO without preferential orientation.

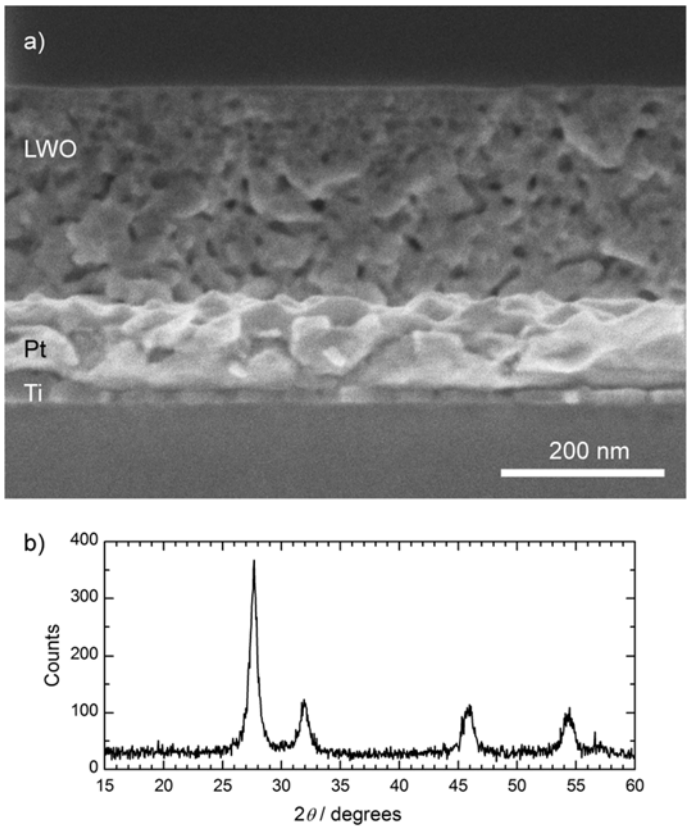

Figure 3. (a) SEM image of LWO thin film deposited from an EDTA-stabilized aqueous solution on platinized Si. 10 layers were deposited with pyrolysis at 500 °C on a hotplate between each layer. The film was finally crystallized at 800 °C for 4 h in air. (b) X-ray diffractogram with grazing incidence θ = 1° of the LWO thin film imaged in (a).

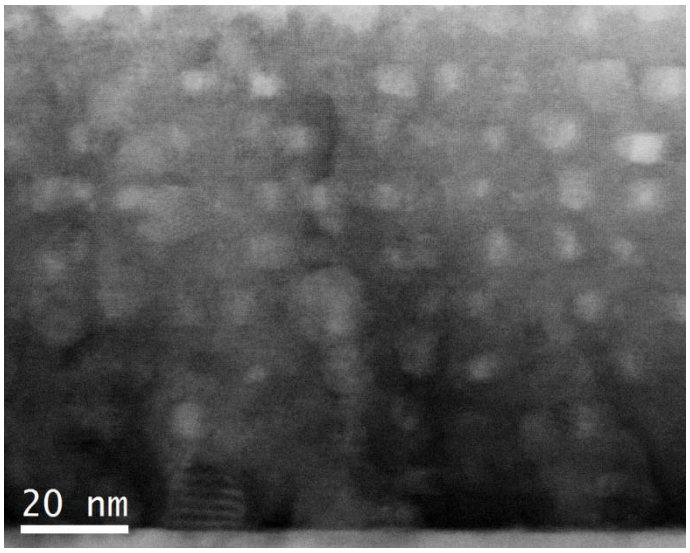

Figure 4. STEM bright field image of an epitaxial BZY film on MgO annealed at 1000 °C. The regular STEM-brighter spots are volumes of lower density (voids), in an otherwise monolithic (single crystal) matrix.

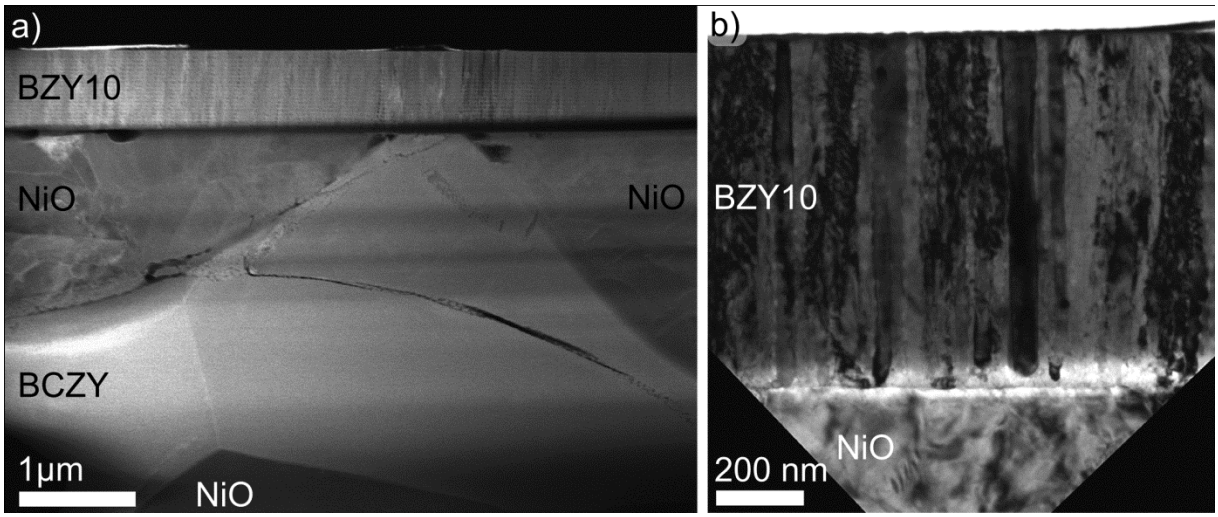

Figure 5. (S)TEM images of BZY film deposited by CSD (20 layers) on a dense BCZY27-NiO anode and annealed at 1000 °C. (a) Overview STEM HAADF image. (b) Higher magnification TEM image of the columnar BZY growth on a NiO part of the anode.

[Two-column image]